

Luminescent Molecular Ag–S Nanocluster $[\text{Ag}_{62}\text{S}_{13}(\text{SBu}^t)_{32}](\text{BF}_4)_4$

Gen Li, Zhen Lei, and Quan-Ming Wang*

State Key Laboratory of Physical Chemistry of Solid Surfaces, Department of Chemistry, College of Chemistry and Chemical Engineering, Xiamen University, Xiamen, Fujian 361005, P. R. China

Received September 26, 2010; E-mail: qmwang@xmu.edu.cn

Abstract: The first observation of luminescence from a structurally well-defined Ag_2S molecular nanocluster is reported. Reaction of $\text{AgSBu}^t/\text{AgBF}_4$ with N_2H_4 in methanol affords the tetracationic cluster $[\text{Ag}_{62}\text{S}_{13}(\text{SBu}^t)_{32}](\text{BF}_4)_4$, which has a core–shell configuration. The 14 silver(I) centers of the $[\text{Ag}_{14}\text{S}_{13}]$ core are in a face-centered cubic arrangement with each edge bridged by a S^{2-} ligand; the core is further connected to the $[\text{Ag}_{48}(\text{SBu}^t)_{32}]$ shell via both Ag–S bonds and $\text{Ag}\cdots\text{Ag}$ interactions. This novel cluster displays intense red emission in both the solid state and solution at room temperature.

High-nuclearity metal clusters are of increasing interest because of their structural diversity and various potential applications.^{1,2} Many organic-agent-protected nanoparticles of noble metals have been reported, and the synthesis of Ag_2S nanocrystals has also been described because of their semiconductor properties.³ Near-IR photoluminescence in Ag_2S quantum dots has been reported,⁴ and visible emissions from silver sulfide–zeolite A composites at low temperature have been observed.⁵ Molecular Ag_2S nanoclusters are of special importance because their well-defined structures facilitate the study of the structural and physical properties without polydispersity effects. While molecular Ag_2S nanoclusters are expected to have interesting optical properties,⁶ there have been no reports in the literature concerning their luminescence behavior. Consequently, structure–property relationships have not been established in terms of luminescence of Ag_2S nanoclusters.

Recent studies have revealed that Ag_2S nanoclusters can be stabilized with surface thiolate ligands exclusively without the ligation of phosphines.^{6,7} In our effort to prepare silver sulfide materials, we have developed a facile synthetic approach to molecular Ag_2S nanoclusters. The heating of the three components AgBF_4 , H_2NNH_2 , and AgSBu^t led to the isolation of a large Ag_2S molecular nanocluster, $[\text{Ag}_{62}\text{S}_{13}(\text{SBu}^t)_{32}](\text{BF}_4)_4$ (**1**). To our surprise, cluster **1** emits bright-red light in both the solid state and solution in addition to its novel structural features. Herein we report the synthesis, crystal structure, and photophysical properties of **1**, and this is the first report of a structurally characterized luminescent Ag_2S nanocluster.

In the formation of **1**, the *tert*-butyl thiolates play two important roles: they not only construct a protecting periphery around the cluster but also act as the origin of S^{2-} . The scission of the S–C bond of tBuS^- releases a S^{2-} ion in the presence of reductive hydrazine. In Ag_2S systems, $\text{S}(\text{SiMe}_3)_2$ and CS_2 have been used as S^{2-} sources, and in cases using $\text{S}(\text{SiMe}_3)_2$ or RSSiMe_3 as the reactants, it was claimed that phosphines are necessary in the preparation even though the products contain no phosphines.^{7b} The composition of **1** was confirmed by NMR spectroscopy and elemental analysis (see the Supporting Information). The presence of BF_4^- counterions was also confirmed by the IR band at 1084 cm^{-1} .

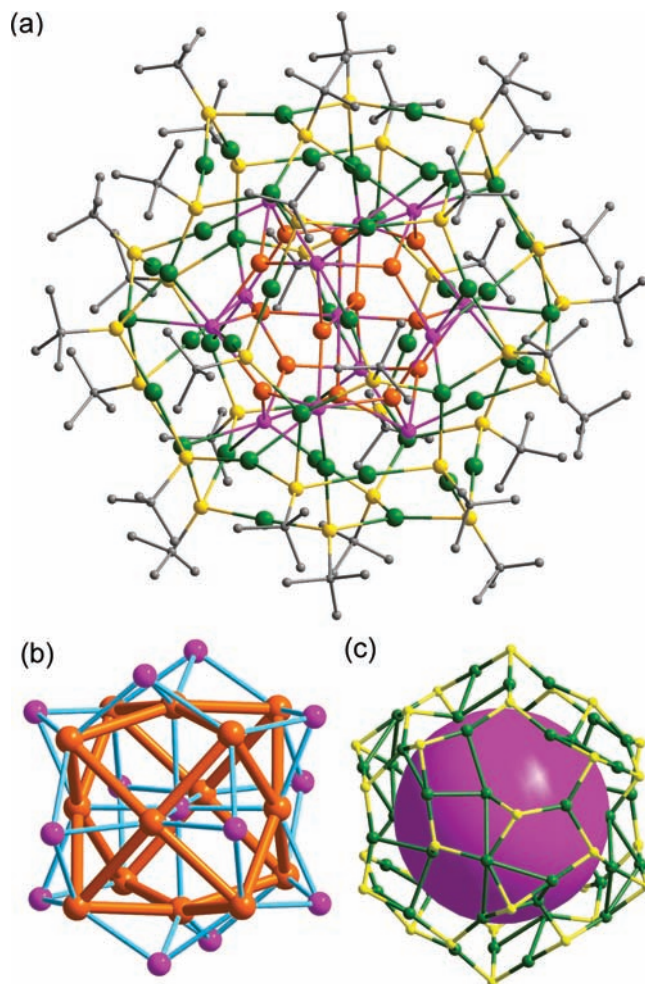


Figure 1. (a) Centrosymmetric structure of the cationic part of $[\text{Ag}_{62}\text{S}_{13}(\text{SBu}^t)_{32}](\text{BF}_4)_4$ (**1**). (b) The $[\text{Ag}_{14}\text{S}_{13}]$ core configuration in **1**. (c) The $\text{Ag}_{48}(\text{SBu}^t)_{32}$ shell structure. The $[\text{Ag}_{14}\text{S}_{13}]$ core and the *tert*-butyl groups have been omitted for clarity, and the artificial large purple sphere shows the inner space occupied by the $[\text{Ag}_{14}\text{S}_{13}]$ core. Color legend: orange, Ag (core); green, Ag (shell); purple, S^{2-} ; yellow, S (thiolate); gray, C.

Single-crystal X-ray structural analysis⁸ revealed that **1** consists of a tetracationic spherical cluster containing 62 silver(I) centers with four BF_4^- serving as counterions (Figure 1a). The cationic cluster is centrosymmetric, with the inversion center located at the S atom in the middle. The complex structure can be understood as a core–shell configuration with a $[\text{Ag}_{14}\text{S}_{13}]$ core (Figure 1b) and a $\text{Ag}_{48}(\text{SBu}^t)_{32}$ shell (Figure 1c). The core contains 14 silver(I) ions and 13 sulfide ions. Eight of the 14 Ag^+ ions form a cubic arrangement, and each of the remaining six Ag^+ ions sits in the center of a tetrasilver square. One sulfide ion is in the center, and each of the remaining 12 S^{2-} ions is located on one of the 12 edges

of the cubane. An alternative description is that six of the 14 Ag^+ ions form an octahedron with each of the remaining eight Ag^+ ions capping a triangular face. As shown in Figure 1b, all 14 silver(I) atoms have similar coordination environments. Every Ag^+ is in the middle of a triangle formed by three S^{2-} , with Ag–S bond lengths in the range 2.531(2)–2.618(2) Å. The central S^{2-} ion is in an almost regular octahedral environment presented by six silver(I) ions, with Ag–S bond lengths from 2.540 to 2.565 Å. The remaining S^{2-} ions function as μ_6 and μ_7 bridges binding both core and shell Ag^+ ions with Ag–S bond lengths in the ranges 2.387(2)–2.877(2) Å and 2.408(2)–2.920(2) Å, respectively.

The shell structure is illustrated in Figure 1c. The shell Ag^+ ions can be classified into two categories: 36 Ag^+ ions are at the surface, and the other 12 are located at the subsurface. All of the thiolate S atoms are triply coordinated to shell silver atoms, with Ag–S bond lengths in the range 2.311(2)–2.579(2) Å; this is quite different from the fact that many μ_2 thiolates are found on the surface of Ag_2S nanoclusters, as reported by Fenske and co-workers.² The thiolates in **1** can be sorted into two types (Figure 2a): type A is coordinated to three surface silver atoms, while type B is ligated to two surface silver atoms and one subsurface silver atom. Thus, the surface of **1** is covered by *tert*-butyl thiolates to form a spherical shape, and the cluster is ~ 2 nm in diameter (Figure 2b). Substantial $\text{Ag}^1 \cdots \text{Ag}^1$ contacts are presented in **1**, with Ag–Ag distances ranging from 2.862(1) to 3.377(1) Å.

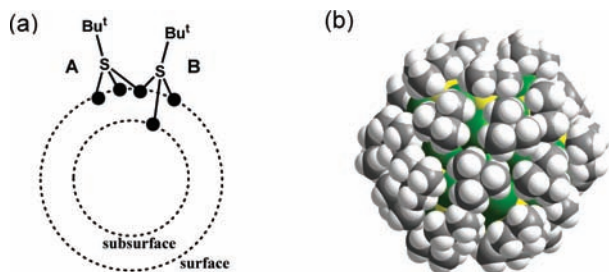


Figure 2. (a) Two kinds of coordination environments of SBU' ligands in **1**. (b) Space-filling representation of the molecular structure of **1** showing the surface coverage by the *tert*-butyl thiolates.

Complex **1** is stable in air. It is soluble in methanol but sparingly soluble in chloroform. At room temperature, the ^1H NMR spectrum of **1** in CD_3OD showed two resonances (1.91 and 1.75 ppm) in a ratio of 5:3, which is consistent with the numbers of the two types of $^t\text{BuS}^-$ ligands (20 type A vs 12 type B). This result indicates that the nanocluster is intact in solution. However, the molecular ion peak was not located in the electrospray ionization mass spectrum because fragmentation occurred during the ionization process.

The electronic absorption spectrum of **1** exhibits two shoulders in the UV region and an absorption in the visible region (Figure 3a). The low-energy band at 543 nm is assigned to the S 3p \rightarrow Ag 5s electronic transition, as a similar assignment was made in a hypothetical Ag_2S monomer.⁹ The excitation spectrum of **1** in MeOH displays a high-energy band in the UV region and two lower-energy bands (497 and 591 nm). The strong visible-light excitation is advantageous for the use of **1** as an emitter in bioapplications. The dissimilarity between the absorption and excitation spectra of **1** suggests that the transition is spin-forbidden. The triplet nature of the excited state was confirmed by lifetime data ($31.7 \pm 0.9 \mu\text{s}$ in the solid state and $1.5 \pm 0.2 \mu\text{s}$ in methanol solution).

Complex **1** emits bright-red light in the solid state under UV or visible irradiation at room temperature with the $\lambda_{\text{em}}^{\text{max}} = 621$ nm. Interestingly, **1** is also intensely emissive in solution, with $\lambda_{\text{em}}^{\text{max}} = 613$ nm. The quantum yield was measured to be 0.014 with rhodamine B in absolute ethanol as the standard (0.69).¹⁰ Phosphine-stabilized tetranuclear silver sulfide clusters are known, and their emissions have been assigned as originating from a ligand-to-metal charge-transfer [$\text{S}^{2-} \rightarrow \text{M}_n$] excited state with mixing of a metal-centered ($d \rightarrow s/d \rightarrow p$) state.¹¹ The red emission from **1** is tentatively assigned as originating from an excited state relating to charge transfer from S 3p to Ag 5s perturbed by $\text{Ag}^1 \cdots \text{Ag}^1$ interactions. Additionally, it is worth noting that a methanol solution of **1** was still brightly emissive after being kept under ambient light for months.

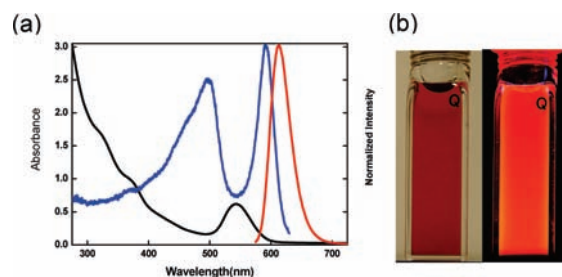


Figure 3. (a) Electronic absorption (black trace), excitation (blue trace), and emission (red trace) spectra of **1**. (b) Photos of emissions from **1** in MeOH at room temperature under ambient light and 365 nm excitation.

In summary, this work has demonstrated that nanocluster **1** is a strong luminophore in both solution and the solid state at room temperature. Further work on revealing the structure–property relationships in Ag_2S nanoclusters is in progress.

Acknowledgment. We acknowledge financial support by the Natural Science Foundation of China (20771091, 20721001, 20973135, and 90922011), the 973 Program (2007CB815301), and NFFTBS (J1030415).

Supporting Information Available: Detailed experimental procedures, characterization data, and crystallographic data (CIF) for **1**. This material is available free of charge via the Internet at <http://pubs.acs.org>.

References

- (1) *Clusters and Colloids: From Theory to Applications*; Schmid, G., Ed.; VCH: Weinheim, Germany, 1994.
- (2) Corrigan, J. F.; Fuhr, O.; Fenske, D. *Adv. Mater.* **2009**, *21*, 1867–1871.
- (3) (a) Huxter, V. M.; Mirkovic, T.; Nair, P. S.; Scholes, G. D. *Adv. Mater.* **2008**, *20*, 2439–2443. (b) Gao, F.; Liu, Q.-Y.; Zhao, D.-Y. *Nano Lett.* **2003**, *3*, 85–88.
- (4) Du, Y.-P.; Xu, B.; Fu, T.; Cai, M.; Li, F.; Zhang, Y.; Wang, Q.-B. *J. Am. Chem. Soc.* **2010**, *132*, 1470–1471.
- (5) Brühwiler, D.; Leiggner, C.; Glauss, S.; Calzaferri, G. *J. Phys. Chem. B* **2002**, *106*, 3770–3777.
- (6) (a) Anson, C. E.; Eichhöfer, A.; Issac, I.; Fenske, D.; Fuhr, O.; Seivillano, P.; Persau, C.; Stalke, D.; Zhang, J.-T. *Angew. Chem., Int. Ed.* **2008**, *47*, 1326–1331. (b) Tang, K.-L.; Xie, X.-J.; Zhang, Y.-H.; Zhao, X.; Jin, X.-L. *Chem. Commun.* **2002**, 1024–1025.
- (7) (a) Ahmar, S.; MacDonald, D. G.; Vijayaratham, N.; Battista, T. L.; Workentin, M. S.; Corrigan, J. F. *Angew. Chem., Int. Ed.* **2010**, *49*, 4422–4424. (b) Fenske, D.; Anson, C. E.; Eichhöfer, A.; Fuhr, O.; Ingendon, A.; Persau, C.; Richert, C. *Angew. Chem., Int. Ed.* **2005**, *44*, 5242–5246.
- (8) Crystal data for $\text{1} \cdot 4\text{MeOH} \cdot 6\text{H}_2\text{O}$: $\text{C}_{128}\text{H}_{288}\text{B}_3\text{F}_{16}\text{S}_{45}\text{Ag}_{62} \cdot 4\text{MeOH} \cdot 6\text{H}_2\text{O}$; $P1$; $a = 20.9194(7)$ Å, $b = 21.4218(4)$ Å, $c = 21.4404(8)$ Å, $\alpha = 91.558(2)^\circ$, $\beta = 118.826(4)^\circ$, $\gamma = 115.036(2)^\circ$; $V = 7295.9(4)$ Å³; $Z = 1$; $T = 173$ K; 74067 reflns measured, 39260 unique ($R_{\text{int}} = 0.0455$); final $R_1 = 0.0581$, $wR_2 = 0.1645$ for 22764 observed reflections [$I > 2\sigma(I)$].
- (9) Brühwiler, D.; Seifert, R.; Calzaferri, G. *J. Phys. Chem. B* **1999**, *103*, 6397–6399.
- (10) Parker, C. A.; Rees, W. T. *Analyst* **1960**, *85*, 587–600.
- (11) Yam, V. W.-W.; Lo, K. K.-W.; Wang, C.-R.; Cheung, K.-K. *Inorg. Chem.* **1996**, *35*, 5116–5117.

JA108684M